PKNOX2 suppresses lung cancer cell proliferation by inhibiting the PI3K/AKT/mTOR axis

MINGLEI SONG, NAN ZHANG, FUMIN CAO and JUNFENG LIU

Department of Thoracic Surgery, The Fourth Hospital of Hebei Medical University, Shijiazhuang, Hebei 050011, P.R. China

Received September 16, 2022; Accepted March 3, 2023

DOI: 10.3892/etm.2023.11917

Abstract. PBX/knotted 1 homeobox 2 (PKNOX2) has been implicated in tumorigenesis; however, its role in lung cancer (LC) remains unknown. The present study thus aimed to examine the expression, regulation, function and clinical implication of PKNOX2 in LC. A series of experiments were performed, including Cell Counting Kit-8 assay, cell cycle analysis, wound-healing assay, Transwell assay, methylation-specific PCR and western blotting. Bioinformatics analysis revealed that PKNOX2 was a LC-related gene, and a decrease in its expression was found in LC tissues from three public datasets. The results of reverse transcription-quantitative PCR assays also confirmed that PKNOX2 mRNA expression was markedly downregulated in LC tissues (n=60, P<0.01) and in five types of LC cell lines, and this was associated with the promoter methylation of PKNOX2. In addition, PKNOX2 expression was significantly associated with tumor invasion (P<0.0001), lymph node metastasis (P=0.0057) and TNM stage (P=0.0003); however, it was not associated with sex, age, pathological type or distant metastasis. The data obtained *in vitro* demonstrated that PKNOX2 silencing promoted LC cell proliferation and inhibited cell cycle arrest, accompanied by an increase in the expression levels of cell cycle-related proteins (cyclinD1, cyclinE1, CDK2 and CDK4), whereas PKNOX2 overexpression exhibited the opposite trend. In addition, PKNOX2 inhibited the migration and invasion of LC cells. Mechanistically, PKNOX2 knockdown activated the PI3K/AKT/mTOR signaling pathway by accelerating the phosphorylation of PI3K, AKT and mTOR, whereas PKNOX2 overexpression inactivated this signaling pathway. In conclusion, the findings of the present study suggested that PKNOX2 may suppress LC cell proliferation by inhibiting the PI3K/AKT/mTOR axis.

Correspondence to: Dr Junfeng Liu, Department of Thoracic Surgery, The Fourth Hospital of Hebei Medical University, 12 Jiankang Road, Shijiazhuang, Hebei 050011, P.R. China
E-mail: liujf@hebmu.edu.cn; 13931152296@163.com

Key words: lung cancer, PKNOX2, cell proliferation, PI3K/AKT/mTOR axis

Introduction

Lung cancer (LC) is one of the most common malignant tumors worldwide, with a high rate of metastasis and high lethality, severely affecting human health (1). Among all LC cases, non-small cell lung cancer (NSCLC) accounts for >85%, while lung adenocarcinoma (LUAD) is the most common subtype of NSCLC at a percentage of 50% (2). Surgical resection, chemotherapy and radiotherapy remain the main methods of treatment for LC (3). Although the survival rate of patients has been prolonged in recent years, the 5-year survival rate of patients with LC remains very low, at only 21% (4). Therefore, there is an urgent for the exploration of the mechanisms responsible for the occurrence and development of LC, and for the identification of early diagnostic biomarkers for obtaining a satisfactory therapeutic effect.

PBX/knotted 1 homeobox 2 (PKNOX2), a member of the three-amino acid loop extension (TALE) family, which is well-known as a nuclear transcription factor (5). The proteins of the TALE family play vital roles in cell growth, differentiation and death (6-8). To date, numerous gaps remain in the knowledge of gene function that need to be filled. Limited research reports that the PKNOX2 gene on chromosome 11 is markedly associated with complex substance dependence on a genome-wide basis in women of European descent (9). Zhang *et al* (10) revealed that PKNOX2 expression was downregulated in gastric cancer (GC), as shown by promoter methylation, and is highly associated with an unsatisfactory prognosis of patients with GC. DNA methylation is critical for the development and progression of LC (11). Various tumor suppressor genes are inhibited by hypermethylation in cancers (12,13). However, there is limited information regarding the role of PKNOX2 in LC.

The phosphatidylinositol 3-kinase (PI3K)/AKT/mechanistic target of rapamycin (mTOR) signaling cascade is crucial in the modulation of cellular proliferation and metabolism (14). The activation of the PI3K/AKT/mTOR pathway is involved in the development of numerous types of cancer, including LC (15). For instance, Zhao *et al* (16) demonstrated that downstream of tyrosine kinase 7 transcript variant 1inhibited LC cell proliferation and migration by negatively regulating the PI3K/AKT/mTOR signaling pathway. Hu *et al* (17) revealed that family with sequence similarity 83 member A promoted the tumorigenesis of NSCLC by facilitating the phosphorylation of PI3K/AKT/mTOR. These findings suggest that this

pathway provides an attractive target for novel anticancer therapies. At present, there are several specific inhibitors of PI3K, AKT and mTOR that have been in development, and are also in various stages of preclinical studies and early clinical trials for NSCLC (18). Thus, to the best of our knowledge, the present study is the first to investigate whether PKNOX2 is involved in the development of LC through the PI3K/AKT/mTOR axis.

Materials and methods

Gene Expression Omnibus (GEO) database and bioinformatics analysis. The expression profiles were downloaded from the GEO database (http://www.ncbi.nlm.nih.gov/geo/; GSE31210 (19), GSE140797 (20) and GSE130779 (21)) and GEPIA2 website (http://gepia2.cancer-pku.cn/, GEPIA-lung adenocarcinoma (LUAD)). In the early stage of this study, we randomly employed the expression profile data of LC from different public datasets (GSE140797, GSE130779 and GEPIA-LUAD) to explore downregulated genes. GEO2R (http://www.ncbi.nlm.nih.gov/geo/geo2r/) was used to identify differentially expressed genes. The biological consequences of genes were explored using Gene Ontology (GO) and Kyoto Encyclopedia of Genes and Genomes (KEGG) enrichment analysis. In order to investigate the relationship between PKNOX2 expression and EGFR and ALK-fusion mutations in LC patients, data from GSE31210 were employed.

Human LC samples and cell culture. A total of 60 paired LC and adjacent normal tissues were collected from Jan 2020 to Jun 2020 at The Fourth Hospital of Hebei Medical University (Shijiazhuang, China). All experiments were approved by the Ethics Committee of The Fourth Hospital of Hebei Medical University (2018MEC160), and written informed consent was obtained from all patients. Patients diagnosed with recurrence and those who received preoperative radiotherapy, chemotherapy, or biotherapy were excluded from the study.

The human bronchial epithelial cell line (HBE) was purchased from CHI Scientific, Inc. The PLA-801D, A549, NCI-H1299, HCC827 and NCI-H1437 cell lines were purchased from iCell Bioscience Inc. The A549 cells were cultured in F-12K medium (Procell Life Science & Technology Co., Ltd.) containing 10% fetal bovine serum (FBS, Zhejiang Tianhang Biotechnology Co., Ltd.). The other cell lines were maintained in RPMI-1640 medium (Beijing Solarbio Science & Technology, Co., Ltd.) supplemented with 10% FBS. All cell lines were incubated at 37˚C in a humidified atmosphere containing 5% CO_2.

Cell transfection. Specific siRNAs targeting PKNOX2 was used to silence PKNOX2 (https://www.ncbi.nlm.nih.gov/nuccore/NM_001382323.2?report=fasta, si-PKNOX2-1, location at 1583-1601; si-PKNOX2-2, location at 430-448; si-PKNOX2-3, location at 1311-1329; si-PKNOX2-1 sense, 5'-GACGAGCUGCAGACGACAATT-3' and antisense, 5'-UUGUCGUCUGCAGCUCGUCTT-3'; si-PKNOX2-2 sense, 5'-GGCUGACAAGCGAGCUGUATT-3' and antisense, 5'-UACAGCUCGCUUGUCAGCCTT-3'; si-PKNOX2-3 sense, 5'-CCAAGAAGAUCAAGUCUCATT-3' and antisense, 5'-UGAGACUUGAUCUUCUUGGTT-3'). The sequence of PKNOX2 (NM_001382323) cDNA was applied to overexpress PKNOX2 (oe-PKNOX2) using pcDNA3.1 plasmid, which was obtained from General Biol Co., Ltd (http://www.generalbiol.com/). si-NC (sense, 5'-UUCUCCGAACGUGUCACG UTT-3' and antisense, 5'-ACGUGACACGUUCGGAGA ATT-3') and empty vector were used as negative controls. The A549 and HCC827 cells were transiently transfected with PKNOX2-silencing or PKNOX2-overexpressing plasmid using Lipofectamine 3000® (Invitrogen; Thermo Fisher Scientific, Inc.).

Reverse transcription-quantitative PCR (RT-qPCR). Total RNA was isolated from the tissues and cultured cells using TRIpure (BioTeke Corporation) according to the manufacturer's protocol. The RNA was reverse transcribed into cDNA using the BeyoRT II M-MLV (Beyotime Institute of Biotechnology). The qPCR assay was performed using SYBR-GREEN reagents (Beijing Solarbio Science & Technology, Co., Ltd.). The thermocycling conditions were shown below: initial denaturation at 94˚C for 5 min, followed by 40 cycles of 94˚C for 20 sec, 60˚C for 30 sec and 72˚C for 40 sec. The mRNA expression was calculated using the $2^{-\Delta\Delta Cq}$ method (22), and β-actin was used as an endogenous control. The PKNOX2-specific primer sequences were as follows: forward, 5'-CTCCTGACGCTG CTGTTT-3'; and reverse, 5'-GTCGCTGTGCATCTTGGT-3'. The β-actin primer sequences were as follows: forward, 5'-TCA TCACCATTGGCAATGAG-3'; and reverse, 5'-CACTGTGTT GGCGTACAGGT3'.

Methylation-specific PCR (MSP). Genomic DNA was obtained from the tissues using the DNA extraction kit (BioTeke Corporation). The EZ-DNA methylation kit (Zymo Research Corp.) was used to modify the genomic DNA. The PKNOX2 MSP primers were designed according to the following method. First, the FASTA sequence of ENST00000298282.14 used was obtained from the URL (https://genome.ucsc.edu/cgi-bin/hgNear?hgsid=1577886959_4A94j58ojWjpxtXTgErSymdKA mcK&near.getSeqHow=promoter&near.proUpSize=2000& near.proDownSize=0&near.proIncludeFiveOnly=on&bool shad.near.proIncludeFiveOnly=0&near.do.getSeq=get+ sequence). Next, we inputted the above sequence into the URL (http://www.urogene.org/cgi-bin/methprimer/methprimer.cgi), clicked the options 'Pick MSP primers' and 'Use CpG island prediction for primer selection', and clicked 'submit'. Last, MSP primers were as follows. The methylated (M) primers used were TAGTATCGGTGATATTTTGGAATTC and ACC TACTCCTACGACAAAAAAACG (Start position: 1607; Product size: 172 bp). The unmethylated (U) primers used were AGTATTGGTGATATTTTGGAATTTG and AAC CTACTCCTACAACAAAAAAACA (Start position: 1608; Product size: 172 bp). The reaction conditions were as follows: initial denaturation at 95˚C for 10 min, followed by 38 cycles of 95˚C for 20 sec, 54˚C for 25 sec and 72˚C for 30 sec. Then, the PCR products were electrophoresed on a 2% agarose gel.

Cell Counting Kit-8 (CCK-8) assay. Cell viability was determined using CCK-8 kits (Beijing Solarbio Science & Technology, Co., Ltd.). The cells were seeded in 96-well plates ($4x10^3$ cells/well) for 0, 24, 48 and 72 h, respectively. Subsequently, CCK-8 solution (10 μl) was added to each well for 2 h, and the OD value was measured at 450 nm.

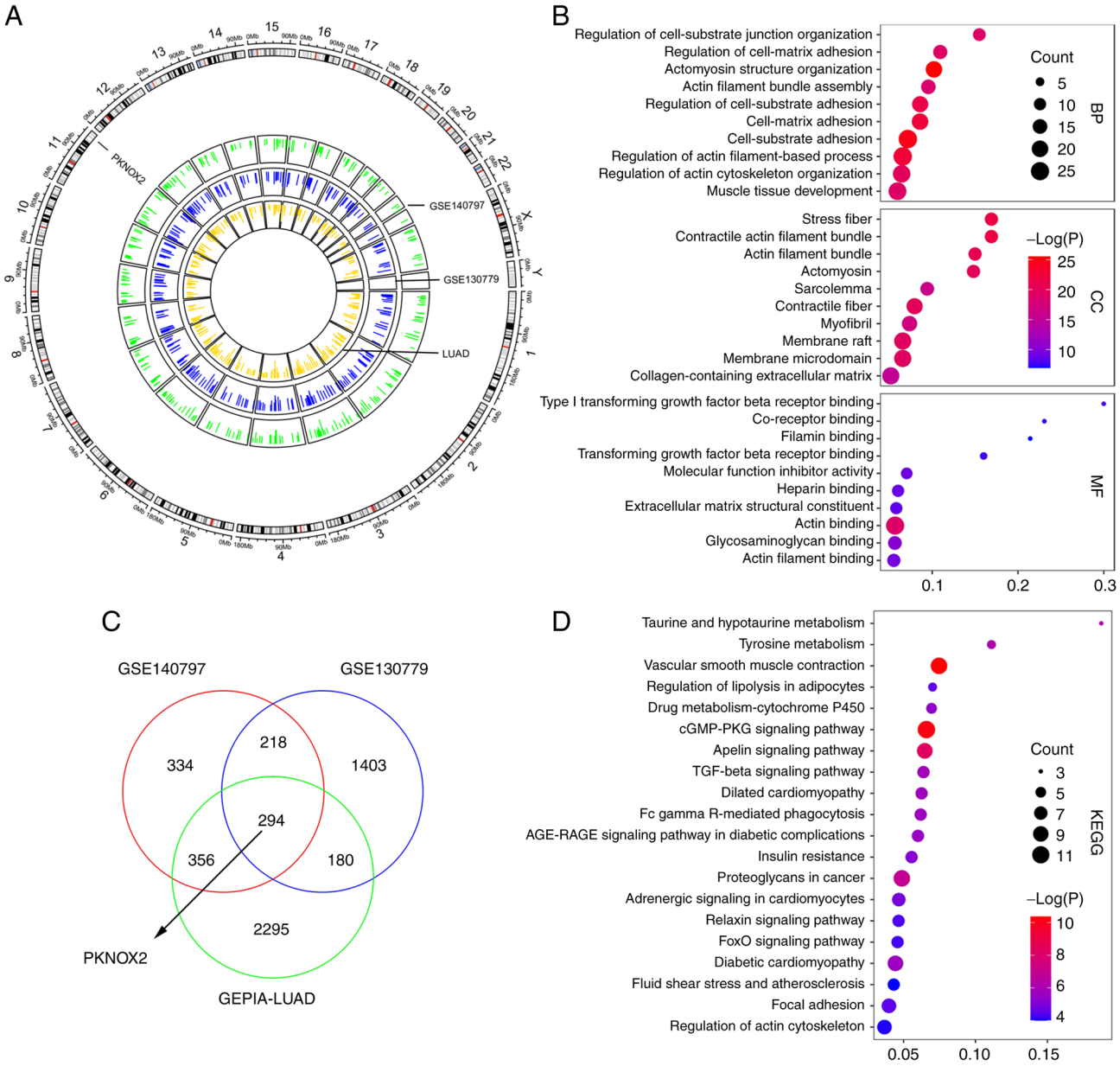

Figure 1. Screening and analysis of downregulated genes in the GSE140797, GSE130779 and GEPIA-LUAD datasets. (A) Circos plot illustrating the distribution of downregulated gene peaks between normal and tumor samples along all chromosomes. (B) Bubble plot illustrating the top 10 Gene Ontology enrichment. (C) Venn diagram of downregulated genes in the above three modules. (D) Bubble plot illustrating the top 20 Kyoto Encyclopedia of Genes and Genomes enrichment results. LUAD, lung adenocarcinoma.

Cell cycle assay. The cells in each group was collected and centrifuged with 150 x g for 5 min. The cells were washed with PBS for twice followed by pre-cooled 70% ethanol 2 h at 4˚C. After washing, the cells were covered with PI and RNase A solution (500 μl, Anhui Leagene Biotechnology) for 30 min at 37˚C in the dark. Subsequently, flow cytometer was used to examine the cell population in G1, S and G2 phases.

Wound healing assay. When the transfected cells were reached 100% confluency, a straight line was scraped using 200 μl pipette tips, and cell debris were removed with serum-free medium. Cells were incubated in serum-free medium at 37˚C for 24 h. Images were captured under a light microscope (Olympus Corporation) at x100 magnification at the indicated time points (0 and 24 h).

Transwell assay. A total of 5x10^4 cells/well in 300 μl serum-free medium were plated in the upper chamber of the Transwell, and the lower chamber was supplemented with 700 μl medium containing 10% FBS. Following incubation for 48 h, the cells were fixed with 4% paraformaldehyde, and stained with 0.5% crystal violet for 5 min. Subsequently, the invasive cell number was counted.

Western blot analysis. The cells were lysed on ice for 5 min with RIPA lysis buffer containing 1% phenylmethanesulfonyl fluoride (PMSF, Beyotime Institute of Biotechnology). Following centrifugation at 1x10^4 x g for 3 min at 4˚C, the BCA assay kit (Beyotime Institute of Biotechnology) was applied to determine the protein concentration. The protein samples were then separated using SDS-PAGE and transferred onto

Table I. Association between PKNOX2 expression and clinicopathological features in LC.

Characteristics	Patients (n=60)	Expression of PKNOX2		P-value
		High (n=30)	Low (n=30)	
Sex				0.795
Male	33	17	16	
Female	27	13	14	
Age, years				0.781
<60	19	10	9	
>60	41	20	21	
Pathological type				>0.99
Adenocarcinoma	55	28	27	
Squamous cell carcinoma	5	2	3	
Tumor invasion				<0.0001[a]
T1	32	25	7	
T2	25	5	20	
T3	3	0	3	
Lymph node metastasis				0.0057[a]
N0	41	26	15	
N1	9	3	61	
N2+N3	10	1	9	
Distant metastasis				>0.99
M0	60	30	30	
M1	0	0	0	
TNM stage				0.0003[a]
I	37	26	11	
II	12	3	9	
III + IV	11	1	10	

[a]P<0.01. PKNOX2, PBX/knotted 1 homeobox 2.

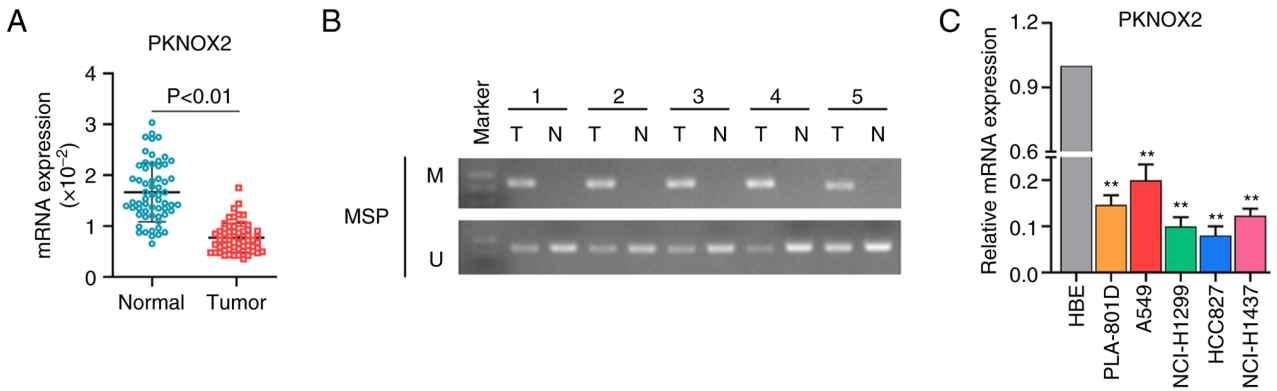

Figure 2. Expression of PKNOX2 in LC tissues and cell lines. (A) The mRNA expression of PKNOX2 in 60 paired LC and para-tumor tissues detected using reverse transcription-quantitative PCR. (B) Methylation-specific PCR was applied to determine the promoter methylation of PKNOX2 in tissue specimens. (C) PKNOX2 mRNA expression in five types of LC cell lines. **P<0.01. PKNOX2, PBX/knotted 1 homeobox 2; LC, lung cancer.

PVDF membranes (Thermo Fisher Scientific, Inc.). After the membranes were blocked with BSA (Biosharp Life Sciences) for 1 h, they were incubated with the respective primary antibodies at 4˚C overnight. The primary antibodies used were anti-PKNOX2 (1:1,000 dilution; Affinity Biosciences, Ltd.), anti-cyclinD1 (1:1,000 dilution; ABclonal Biotech Co., Ltd.), anti-cyclinE1 (1:1,000 dilution; ABclonal Biotech Co., Ltd.), anti-CDK2 (1:1,000 dilution; ABclonal Biotech Co., Ltd.), anti-CDK4 (1:1,000 dilution; ABclonal Biotech Co., Ltd.), anti-PI3K p85α (1:1,000 dilution; ABclonal Biotech Co.,

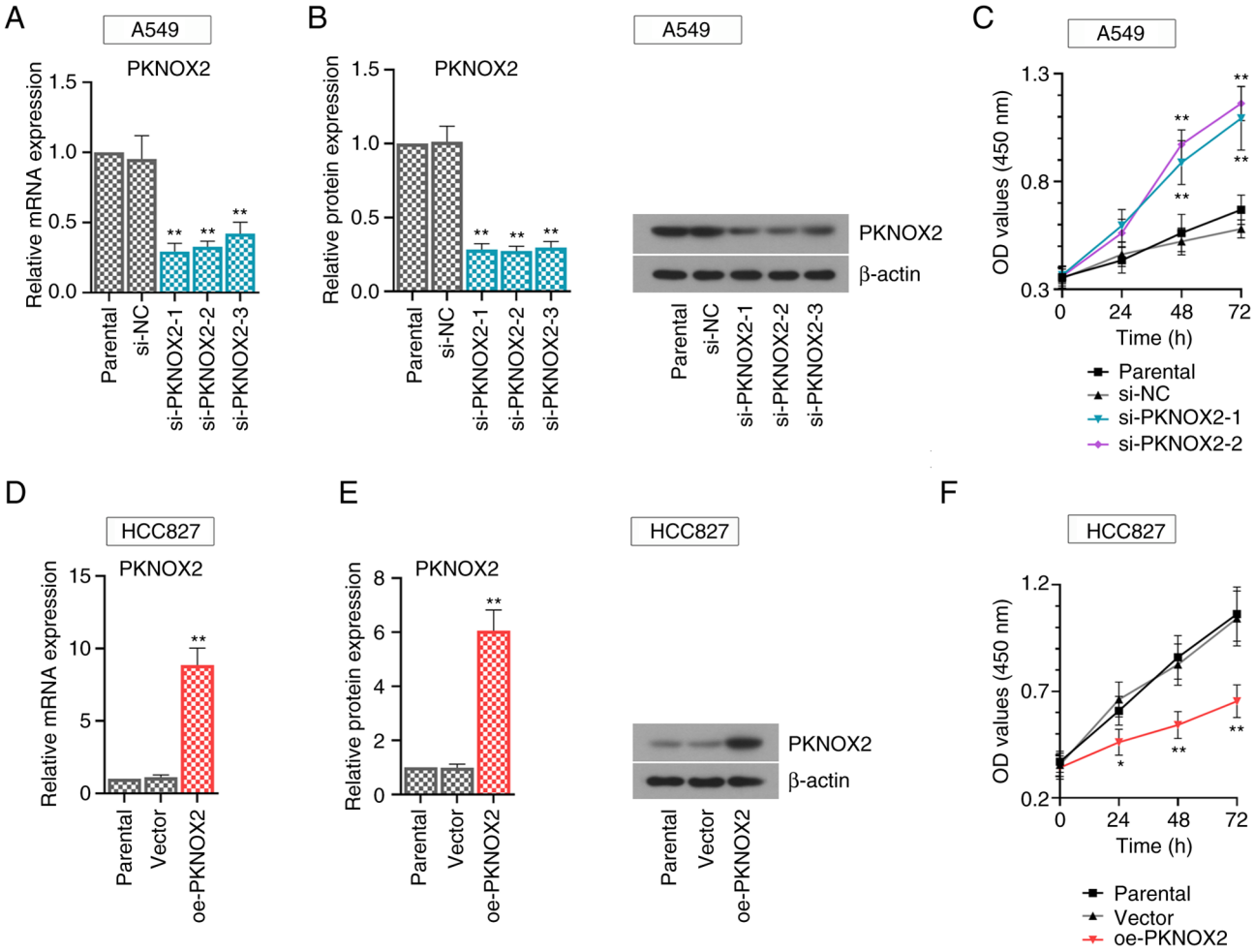

Figure 3. PKNOX2 inhibits lung cancer cell growth. (A and B) PKNOX2 silencing in A549 cells and (D and E) PKNOX2 overexpression in HCC827 cells were confirmed using reverse transcription-quantitative PCR and western blot analysis. (C and F) CCK-8 assay was applied to assess the viability of A549 and HCC827 cells. *P<0.05 and **P<0.01 vs. si-NC or vector. PKNOX2, PBX/knotted 1 homeobox 2.

Ltd.), anti-PI3K p110α (1:1,000 dilution; Affinity Biosciences, Ltd.), anti-p-AKT (1:2,000 dilution; Affinity Biosciences, Ltd.), anti-AKT (1:1,000 dilution; Affinity Biosciences, Ltd.), anti-p-mTOR (1:2,000 dilution; Affinity Biosciences, Ltd.), anti-mTOR antibody (1:1,000 dilution; Affinity Biosciences, Ltd.). Subsequently, the membranes were incubated with HRP-labeled goat anti-rabbit IgG (1:10,000 dilution; Affinity Biosciences, Ltd.) for 40 min at 37˚C. Subsequently, enhanced chemiluminescence (ECL) was added to the membranes, and the bands were analyzed using Gel-Pro Analyzer software (Media Cybernetics, Inc.).

Statistical analysis. All statistical analyses were performed using GraphPad Prism 8.0 (GraphPad Software; Dotmatics). A paired Student's t-test was used to examine the differences when comparing paired tumor and adjacent tissues. The unpaired Student's t-test was used when two independent groups were being compared. The Chi-squared test, Chi-squared with Yates' correction, or Fisher's exact test were applied to assess the associations between PKNOX2 expression and the clinicopathological parameters of the patients with LC. One-way analysis of variance followed by the Bonferroni post hoc test were employed for analyses involving more than two groups. The experiments were repeated at least three times, and data from independent experiments are presented as the mean ± standard deviation. P<0.05 was considered to indicate a statistically significant difference.

Results

Bioinformatics evaluation of LC-related downregulated genes in public datasets. Data employed from three public datasets, GSE140797, GSE130779 and GEPIA-LUAD, were applied for the bioinformatics analysis. GSE140797 and GSE130779 contained 7- and 8-paired LC and para-tumor tissue samples, respectively. There were 483 LC and 347 normal samples in the GEPIA-LUAD dataset. Circos plot demonstrated the distribution of downregulated gene peaks between normal and tumor samples along all chromosomes (Fig. 1A). The outer ring sections refers to the chromosomes. The inner track reveals the downregulated genes in the GSE140797, GSE130779 and GEPIA-LUAD datasets. A Venn diagram illustrated 294 overlapping downregulated genes in the aforementioned three modules (Fig. 1C). To gain further insight into the selected genes, GO function (Fig. 1B) and KEGG pathway enrichment analyses (Fig. 1D) were performed. The results revealed a tendency for enrichment in different pathways, suggesting that different modules may perform various

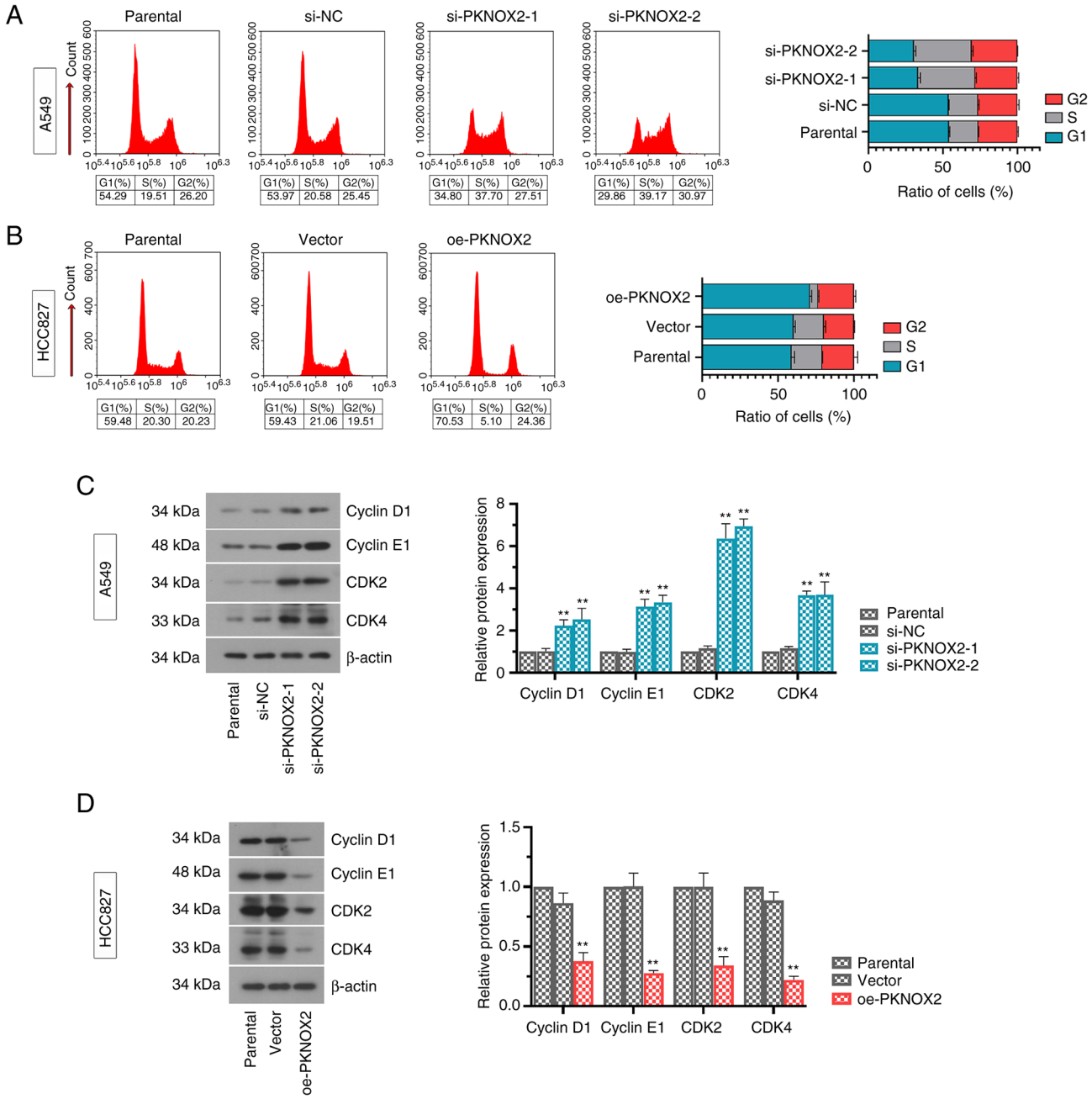

Figure 4. PKNOX2 induces cell cycle arrest in lung cancer cells. (A and B) Flow cytometry was performed to determine cell cycle distribution in A549 and HCC827 cells. The overexpression of PKNOX2 blocked cell cycle progression in the G1 phase, while PKNOX2 knockdown exerted the opposite effect. (C and D) Expression levels of representative cell cycle-related proteins were evaluated using western blot analysis. **P<0.01 vs. si-NC or vector. PKNOX2, PBX/knotted 1 homeobox 2.

functions. The biological processes (BP), cellular components (CC) and molecular functions (MF) were associated with cell-substrate adhesion, contractile fiber and actin binding, respectively. These 10 enriched pathways were related to vascular smooth muscle contraction and the cyclic guanosine monophosphate/protein kinase G signaling pathway.

Expression and promoter methylation of PKNOX2 in LC tissues and cells. A total of 60 pairs of LC tissues and adjacent normal tissues were collected for assessing the expression level of PKNOX2. The results of RT-qPCR indicated that PKNOX2 was expression downregulated in LC tissues compared with normal tissues (Fig. 2A). As shown in Fig. 2B, the promoter methylation of PKNOX2 was ubiquitous in the LC tissues, whereas the adjacent normal tissues were not methylated. Subsequently, PKNOX2 mRNA expression was determined in five types of LC cell lines (PLA-801D, A549, NCI-H1299, HCC827 and NCI-H1437) and in the HBE cell line. Similarly, the mRNA expression of PKNOX2 was significantly decreased in LC cell lines in contrast to that in the HBE cells (Fig. 2C).

Subsequently, the present study analyzed the association between PKNOX2 expression and the clinicopathological parameters of patients with LC. The results revealed that the decreased expression of PKNOX2 was markedly associated with tumor invasion (P<0.0001), lymph node metastasis (P=0.0057) and TNM stage (P=0.0003); however, it was not

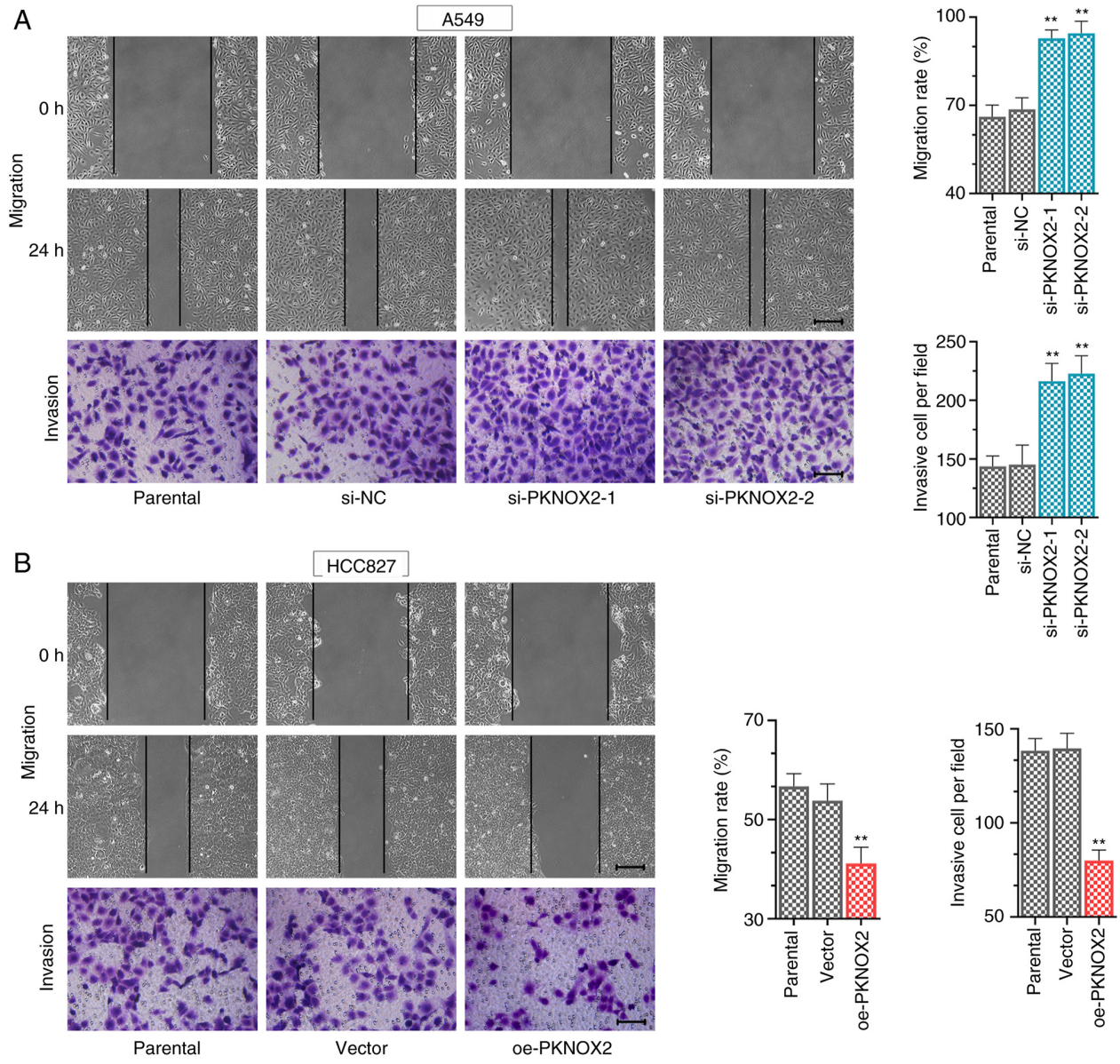

Figure 5. PBX/knotted 1 homeobox 2 suppresses cell migration and invasion. (A and B) Wound healing (scale bar, 200 μm) and Transwell (scale bar, 100 μm) assays were used to detect the ability of cells to migrate and invade. **P<0.01 vs. si-NC or vector.

associated with sex, age, pathological type, or distant metastasis (Table I). In addition, data from GSE31210 showed that PKNOX2 was downregulated in EGFR+ (Fig. S1A, n=127) or ALK-fusion+ (Fig. S1B, n=11) LC tissues compared with that in normal tissues (n=20).

PKNOX2 inhibits LC cell growth. Functional assays were carried out using the A549 cells with a relatively high PKNOX2 expression and with the HCC827 cells, with a relatively low expression. To avoid off-target effects, three small interference RNA sequences (si-PKNOX2-1~3) were synthesized in this study. The results of real-time PCR and western blot assays demonstrated the efficacy of gene transfer. PKNOX2 expression was effectively suppressed in the PKNOX2-silenced A549 cells (Fig. 3A and B). Consistently, PKNOX2 expression was markedly increased in the PKNOX2-overexpressing HCC827 cells (Fig. 3D and E). The si-PKNOX2-1/2 showed relatively superior knockdown efficiency, and they were applied to perform further functional experiments. It was found that PKNOX2 knockdown promoted LC cell growth, while PKNOX2 overexpression exerted the opposite effects (Fig. 3C and F).

PKNOX2 blocks the cell cycle at the G1 phase. As shown in Fig. 4A and B, the silencing of PKNOX2 markedly reduced the ratio of cells in the G1 phase. On the contrary, the overexpression of PKNOX2 successfully arrested the cells at the G1 phase. Consistent with these results, the protein levels of G1 cell cycle promoters (cyclinD1, cyclinE1, CDK2 and CDK4) were significantly increased under the condition of PKNOX2 silencing, while the overexpression of PKNOX2 decreased these expression levels (Fig. 4C and D).

PKNOX2 suppresses cell migration and invasion. The data of wound healing and Transwell assays revealed that PKNOX2 knockdown increased the LC cell migratory and invasive

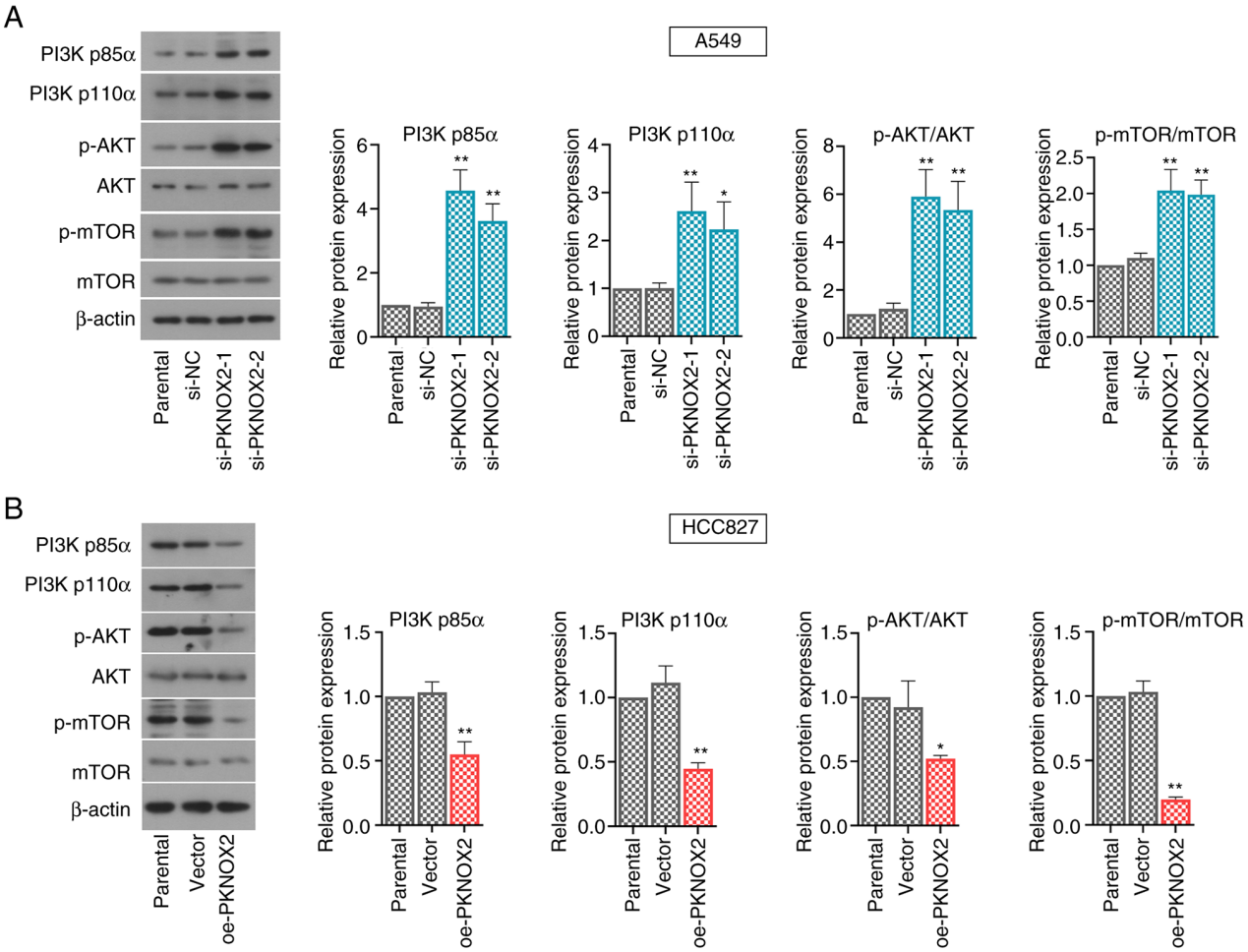

Figure 6. PKNOX2 inactivates the PI3K/AKT/mTOR signaling. Western blot analysis of PI3K p85α, PI3K p110α, p-AKT, AKT, p-mTOR and mTOR in (A) PKNOX2-silenced A549 cells and (B) in PKNOX2-overexpressing HCC827 cells. *P<0.05 and **P<0.01 vs. si-NC or vector. PKNOX2, PBX/knotted 1 homeobox 2.

abilities (Fig. 5A), whilst PKNOX2 overexpression exerted the opposite effect (Fig. 5B).

PKNOX2 represses the PI3K/AKT/mTOR pathway. A number of signaling pathways, including the PI3K/AKT/mTOR pathway, play vital roles in regulating cell proliferation. The present study demonstrated that PKNOX2 silencing accelerated the phosphorylation of PI3K, AKT and mTOR, whilst the levels of phosphorylated PI3K, AKT and mTOR were markedly suppressed by PKNOX2 overexpression (Fig. 6A and B).

Discussion

In contemporary society, LC remains one of the diseases threatening human life. Thus, it is of utmost importance to explore antitumor therapy for LC. Genetic and epigenetic alterations can be involved in the occurrence and development of LC via the activation of growth-promoting pathways and the inhibition of tumor suppressor pathways. Among the epigenetic alterations, the abnormal DNA methylation of promoter CpG islands can repress the transcription of downstream genes, and tumor suppressor genes can be inactivated through this mechanism (23). In the present study, it was first demonstrated that PKNOX2 expression was significantly downregulated in the tissues of patients with LC and in LC cells, which was associated with the promoter methylation of PKNOX2. Additionally, the decreased expression of PKNOX2 was associated with an increased malignant degree, including tumor invasion, lymph node metastasis and TNM stage. EGFR and ALK mutations are major genetic abnormalities in LC. The PKNOX2 expression was reduced in EGFR^{+} or ALK-fusion+ LC tissues, suggesting that PKNOX2 may be a molecular target for EGFR and ALK. Based on these findings, it was hypothesized that PKNOX2 may be a crucial factor affecting LC progression.

Experiments *in vitro* demonstrated that the knockdown of PKNOX2 contributed to the tumor growth of LC A549 cells, as evidenced using cell viability assay. On the other hand, PKNOX2 overexpression markedly inhibited the proliferation of LC HCC827 cells. In addition, it was observed that PKNOX2 increased the number of cells in the G1 phase and decreased the population of cells in the S phase, which indicated that it can block the transition of cells from the G1 to the S phase. At the same time, as was expected, PKNOX2 markedly inhibited G1 cell cycle promoter (cyclinD1, cyclinE1, CDK2 and CDK4) protein expression. It has been reported that CyclinD1 and CDK4 function as critical positive regulators promoting cell cycle progression, forming a cyclinD1-CDK4 complex that

regulates G1/S restriction points (24-27). Similarly, cyclinE1 is usually overexpressed in a variety of cancers and is related to cancer cell proliferation. It affects cell proliferation by activating CDK2 and promotes the cell to pass through the G1/S limiting node (28-30). According to these results, PKNOX2 suppressed cell proliferation by blocking the cell cycle at the G1 phase.

Furthermore, the present study investigated the relevant mechanisms through which PKNOX2 inhibited LC cell growth. Previous studies have proven that the PI3K/AKT/mTOR pathway plays a critical mediating role in numerous biological processes, such as cell proliferation (31-33). PI3K is a heterodimer composed of the regulatory subunit p85 and catalytic subunit p110, which is activated by a variety of cytokines through phosphorylation, and participates in cell growth and survival (34). AKT is a crucial molecule downstream of PI3K, and its hyperphosphorylation is closely related to the proliferation of LC cells. Once AKT is hyperphosphorylated, it can activate a number of downstream targets in the cytoplasm and nucleus, promoting cell growth (35). Furthermore, mTOR is a key substrate of AKT, and activated mTOR can also lead to cell growth (36). The present study revealed that PKNOX2 silencing markedly enhanced the activation of the PI3K/AKT/mTOR pathway, as evidenced by the increased phosphorylation of these proteins. By contrast, PKNOX2 overexpression inactivated the PI3K/AKT/mTOR axis. Moreover, other studies have found that PKNOX2 can transcriptionally activate IGFBP5 in GC cells (10), IGFBP5 can repress LC cell proliferation (37), and IGFBP5 can suppress the activation of PI3K/AKT signaling in prostate cancer (38). These findings also suggest that PKNOX2 may modulate the PI3K/AKT pathway. Taken together, the PKNOX2-mediated suppression of tumor growth may be, at least partly, attributed to the inactivation of the PI3K/AKT/mTOR pathway, which is critical for the initiation and progression of LC.

The limitations of the current study are as follows: i) Since the differences in PKNOX2 expression of LC cell lines in Fig. 2C are not drastic, we will perform do knockdown and overexpression PKNOX2 at the same time in A549 and HCC827 cells in future studies. ii) This study lacks *in vivo* experiments and colony formation assays. iii) This is a basic research to explore the function of PKNOX2 in LC, so as to provide new perspectives and tips for the treatment of LC. It is still uncertain how to increase the expression of PKNOX2 in a clinical setting, which is a challenge for us.

In conclusion, the present study demonstrated that PKNOX2 expression was downregulated in LC tissues and LC cell lines, which was associated with the promoter methylation of PKNOX2. PKNOX2 targets the PI3K/AKT/mTOR pathway to modulate LC cell growth. The data presented herein underscore the crucial roles of PKNOX2 in LC and its therapeutic value.

Acknowledgements

Not applicable.

Funding

No funding was received.

Availability of data and materials

The datasets used and/or analyzed during the current study are available from the corresponding author on reasonable request.

Authors' contribution

MS wrote this article. MS, NZ and FC performed experiments and analyzed data. MS and JL confirm the authenticity of all the raw data. JL designed this study and polished the article. All authors read and approved the final manuscript.

Ethics approval and consent to participate

All experiments were approved by the Ethics Committees of The Fourth Hospital of Hebei Medical University (2018MEC160), and written informed consent was obtained from patients.

Patient consent for publication

Not applicable.

Competing interests

The authors declare that they have no competing interests.

References

1. Torre LA, Siegel RL and Jemal A: Lung cancer statistics. Adv Exp Med Biol 893: 1-19, 2016.
2. Mao Y, Yang D, He J and Krasna MJ: Epidemiology of lung cancer. Surg Oncol Clin N Am 25: 439-445, 2016.
3. Turner MC, Andersen ZJ, Baccarelli A, Diver WR, Gapstur SM, Pope CAP III, Prada D, Samet J, Thurston G and Cohen A: Outdoor air pollution and cancer: An overview of the current evidence and public health recommendations. CA Cancer J Clin 25: 10.3322/caac.21632, 2020.
4. Siegel RL, Miller KD, Fuchs HE and Jemal A: Cancer statistics, 2021. CA Cancer J Clin 71: 7-33, 2021.
5. Imoto I, Sonoda I, Yuki Y and Inazawa J: Identification and characterization of human PKNOX2, a novel homeobox-containing gene. Biochem Biophys Res Commun 287: 270-276, 2001.
6. Moens CB and Selleri L: Hox cofactors in vertebrate development. Dev Biol 291: 193-206, 2006.
7. Capellini TD, Di Giacomo G, Salsi V, Brendolan A, Ferretti E, Srivastava D, Zappavigna V and Selleri L: Pbx1/Pbx2 requirement for distal limb patterning is mediated by the hierarchical control of Hox gene spatial distribution and Shh expression. Development 133: 2263-2273, 2006.
8. Shah N, Wang J, Selich-Anderson J, Graham G, Siddiqui H, Li X, Khan J and Toretsky J: PBX1 is a favorable prognostic biomarker as it modulates 13-cis retinoic acid-mediated differentiation in neuroblastoma. Clin Cancer Res 20: 4400-4412, 2014.
9. Chen X, Cho K, Singer BH and Zhang H: The nuclear transcription factor PKNOX2 is a candidate gene for substance dependence in European-origin women. PLoS One 6: e16002, 2011.
10. Zhang L, Li W, Cao L, Xu J, Qian Y, Chen H, Zhang Y, Kang W, Gou YH, Wong CC and Yu J: PKNOX2 suppresses gastric cancer through the transcriptional activation of IGFBP5 and p53. Oncogene 38: 4590-4604, 2019.
11. Banno K, Kisu I, Yanokura M, Tsuji K, Masuda K, Ueki A, Kobayashi Y, Yamagami W, Nomura H, Tominaga E, *et al*: Epimutation and cancer: A new carcinogenic mechanism of Lynch syndrome (Review). Int J Oncol 41: 793-797, 2012.
12. Wu JE, Wu YY, Tung CH, Tsai YT, Chen HY, Chen YL and Hong TM: DNA methylation maintains the CLDN1-EPHB6-SLUG axis to enhance chemotherapeutic efficacy and inhibit lung cancer progression. Theranostics 10: 8903-8923, 2020.

13. Zheng Y, Wang Z, Wei S, Liu Z and Chen G: Epigenetic silencing of chemokine CCL2 represses macrophage infiltration to potentiate tumor development in small cell lung cancer. Cancer Lett 499: 148-163, 2021.
14. Tan AC: Targeting the PI3K/Akt/mTOR pathway in non-small cell lung cancer (NSCLC). Thorac Cancer 11: 511-518, 2020.
15. Polivka J Jr and Janku F: Molecular targets for cancer therapy in the PI3K/AKT/mTOR pathway. Pharmacol Ther 142: 164-175, 2014.
16. Zhao H, Chen G, Ye L, Yu H, Li S and Jiang WG: DOK7V1 influences the malignant phenotype of lung cancer cells through PI3K/AKT/mTOR and FAK/paxillin signaling pathways. Int J Oncol 54: 381-389, 2019.
17. Hu H, Wang F, Wang M, Liu Y, Wu H, Chen X and Lin Q: FAM83A is amplified and promotes tumorigenicity in non-small cell lung cancer via ERK and PI3K/Akt/mTOR pathways. Int J Med Sci 17: 807-814, 2020.
18. Alzahrani AS: PI3K/Akt/mTOR inhibitors in cancer: At the bench and bedside. Semin Cancer Biol 59: 125-132, 2019.
19. Okayama H, Kohno T, Ishii Y, Shimada Y, Shiraishi K, Iwakawa R, Furuta K, Tsuta K, Shibata T, Yamamoto S, *et al*: Identification of genes upregulated in ALK-positive and EGFR/KRAS/ALK-negative lung adenocarcinomas. Cancer Res 72: 100-111, 2012.
20. Liang J, Li H, Han J, Jiang J, Wang J, Li Y, Feng Z, Zhao R, Sun Z, Lv B and Tian H: Mex3a interacts with LAMA2 to promote lung adenocarcinoma metastasis via PI3K/AKT pathway. Cell Death Dis 11: 614, 2020.
21. He F, Huang L, Xu Q, Xiong W, Liu S, Yang H, Lu W, Xiao R, Hu Z and Cai L: Microarray profiling of differentially expressed lncRNAs and mRNAs in lung adenocarcinomas and bioinformatics analysis. Cancer Med 9: 7717-7728, 2020.
22. Livak KJ and Schmittgen TD: Analysis of relative gene expression data using real-time quantitative PCR and the 2(-Delta Delta C(T)) method. Methods 25: 402-408, 2001.
23. Ushijima T: Detection and interpretation of altered methylation patterns in cancer cells. Nat Rev Cancer 5: 223-231, 2005.
24. Duan PJ, Zhao JH and Xie LL: Cul4B promotes the progression of ovarian cancer by upregulating the expression of CDK2 and CyclinD1. J Ovarian Res 13: 76, 2020.
25. Li S, Ma YM, Zheng PS and Zhang P: GDF15 promotes the proliferation of cervical cancer cells by phosphorylating AKT1 and Erk1/2 through the receptor ErbB2. J Exp Clin Cancer Res 37: 80, 2018.
26. Sun HB, Han XL, Zhong M and Yu DJ: Linc00703 suppresses non-small cell lung cancer progression by modulating CyclinD1/CDK4 expression. Eur Rev Med Pharmacol Sci 24: 6131-6138, 2020.
27. Xi X, Teng M, Zhang L, Xia L, Chen J and Cui Z: MicroRNA-204-3p represses colon cancer cells proliferation, migration, and invasion by targeting HMGA2. J Cell Physiol 235: 1330-1338, 2020.
28. Li X, Zhang Q, Fan K, Li B, Li H, Qi H, Guo J, Cao Y and Sun H: Overexpression of TRPV3 correlates with tumor progression in non-small cell lung cancer. Int J Mol Sci 17: 437, 2016.
29. Ratschiller D, Heighway J, Gugger M, Kappeler A, Pirnia F, Schmid RA, Borner MM and Betticher DC: Cyclin D1 overexpression in bronchial epithelia of patients with lung cancer is associated with smoking and predicts survival. J Clin Oncol 21: 2085-2093, 2003.
30. Keum JS, Kong G, Yang SC, Shin DH, Park SS, Lee JH and Lee JD: Cyclin D1 overexpression is an indicator of poor prognosis in resectable non-small cell lung cancer. Br J Cancer 81: 127-132, 1999.
31. Reddy D, Kumavath R, Ghosh P and Barh D: Lanatoside C induces G2/M cell cycle arrest and suppresses cancer cell growth by attenuating MAPK, Wnt, JAK-STAT, and PI3K/AKT/mTOR signaling pathways. Biomolecules 27: 792, 2019.
32. Zhang HQ, Xie XF, Li GM, Chen JR, Li MT, Xu X, Xiong QY, Chen GR, Yin YP, Peng F, *et al*: Erianin inhibits human lung cancer cell growth via PI3K/Akt/mTOR pathway in vitro and in vivo. Phytother Res 35: 4511-4525, 2021.
33. Zhao YY, Jia J, Zhang JJ, Xun YP, Xie SJ, Liang JF, Guo HG, Zhu JZ, Ma SL and Zhang SR: Inhibition of histamine receptor H3 suppresses the growth and metastasis of human non-small cell lung cancer cells via inhibiting PI3K/Akt/mTOR and MEK/ERK signaling pathways and blocking EMT. Acta Pharmacol Sin 42: 1288-1297, 2021.
34. Sarris EG, Saif MW and Syrigos KN: The biological role of PI3K pathway in lung cancer. Pharmaceuticals (Basel) 5: 1236-1264, 2012.
35. Tsurutani J, Fukuoka J, Tsurutani H, Shih JH, Hewitt SM, Travis WD, Jen J and Dennis PA: Evaluation of two phosphorylation sites improves the prognostic significance of Akt activation in non-small-cell lung cancer tumors. J Clin Oncol 24: 306-314, 2006.
36. Ekman S, Wynes MW and Hirsch FR: The mTOR pathway in lung cancer and implications for therapy and biomarker analysis. J Thorac Oncol 7: 947-953, 2012.
37. Galvan A, Colombo F, Noci S, Pazzaglia S, Mancuso M, Manenti G, Broman KW, Saran A and Dragani TA: The Lsktm1 locus modulates lung and skin tumorigenesis in the mouse. G3 (Bethesda) 2: 1041-1046, 2012.
38. Chen X, Yu Q, Pan H, Li P, Wang X and Fu S: Overexpression of IGFBP5 enhances radiosensitivity through PI3K-AKT pathway in prostate cancer. Cancer Manag Res 12: 5409-5418, 2020.